

54th SME North American Manufacturing Research Conference (NAMRC 54, 2026)

An LLM-Assisted Multi-Agent Control Framework for Roll-to-Roll Manufacturing Systems

 Jiachen Li^a, Shihao Li^a, Christopher Martin^a, Zijun Chen^a, Dongmei Chen^a, Wei Li^{a,*}
^aWalker Department of Mechanical Engineering, University of Texas at Austin

Abstract

Roll-to-roll manufacturing requires precise tension and velocity control to ensure product quality, yet controller commissioning and adaptation remain time-intensive processes dependent on expert knowledge. This paper presents an LLM-assisted multi-agent framework that automates control system design and adaptation for R2R systems while maintaining safety. The framework operates through five phases: system identification from operational data, automated controller selection and tuning, sim-to-real adaptation with safety verification, continuous monitoring with diagnostic capabilities, and periodic model refinement. Experimental validation on a R2R system demonstrates successful tension regulation and velocity tracking under significant model uncertainty, with the framework achieving performance convergence through iterative adaptation. The approach reduces manual tuning effort while providing transparent diagnostic information for maintenance planning, offering a practical pathway for integrating AI-assisted automation in manufacturing control systems.

© 2026 The Authors. Published by Elsevier Ltd. This is an open access article under the CC BY-NC-ND license

<http://creativecommons.org/licenses/by-nc-nd/4.0/>

Peer-review under responsibility of the scientific committee of the NAMRI/SME.

Keywords: Large language models; Roll-to-roll manufacturing; Multi-agent ; Sim-to-real adaptation; Tension control

Nomenclature

E	Modulus (N/m ²)
A	Cross-sectional area (m ²)
R_i	Radius of roller i (m)
J_i	Moment of inertia of roller i (kg·m ²)
f_i	Friction coefficient of motor i (N·m·s·rad ⁻¹)
L_i	Length of web span i (m)
b_i	Disturbance coefficient of motor i
$x(t)$	State vector
$u(t), u_k$	Control input
$y(t), y_k$	Measured output
T_i	Web tension in span i (N)
v_i	Linear velocity of roller i (m·s ⁻¹)
v_0	Unwinding velocity (m·s ⁻¹)

v_i^r	Reference velocity of roller i (m·s ⁻¹)
ω_i	Angular velocity of roller i (rad·s ⁻¹)
u_i	Control torque applied to motor i (N·m)
θ	System parameter vector

1. Introduction

Advanced Roll-to-roll (R2R) manufacturing enables high-volume, cost-effective production of flexible electronics, printed sensors, and functional films [1]. Maintaining precise web tension and velocity control remains critical for product quality [2], with tension variations directly causing defects such as wrinkles, misalignment, and material damage [3]. The core manufacturing challenge lies in managing strongly coupled tension-velocity dynamics while accommodating time-varying parameters from changing roll radius, material property variations, and environmental conditions [4]. Current industrial practice relies on experienced operators and control engineers for manual tuning, requiring time and expertise [5]—particularly

* Corresponding author. Tel.: +1-512-471-7174

 E-mail address: weili@austin.utexas.edu (Wei Li).

problematic when transitioning between product grades or commissioning new production lines.

Large language models (LLMs) offer promising capabilities for automating engineering tasks through natural language reasoning and code generation [6]. Retrieval-Augmented Generation (RAG) further enhances these capabilities by enabling LLMs to dynamically access external knowledge bases [7]. Unlike conventional LLMs that rely only on static pre-training, RAG incorporates dynamic retrieval during inference [8], improving contextual accuracy and reducing wrong outputs by grounding responses in domain-specific information. However, their application to manufacturing control faces critical practical barriers: ensuring operational safety and constraint satisfaction [9], addressing the gap between simulation models and physical systems [10], and maintaining transparent decision-making required in production environments [11, 12]. The question for manufacturing practitioners is whether LLM capabilities can be harnessed to reduce commissioning time and operational burden while maintaining the reliability standards required in industrial settings.

This work proposes an LLM-assisted framework for R2R control that approaches these manufacturing requirements through simulation-validated adaptation. The framework employs specialized agents for system identification, controller design, adaptive tuning, and process monitoring—each operating within rigorous safety constraints. All proposed control modifications undergo simulation validation before deployment to production equipment. The approach delivers: (1) RAG-based knowledge infrastructure that grounds LLM reasoning in control theory and R2R manufacturing domain expertise; (2) automated controller selection and tuning methodology with built-in safety verification; (3) intelligent monitoring that implementation guidelines for manufacturing practitioners; (4) experimental demonstration of successful deployment despite significant model uncertainty.

Section 2 reviews relevant literature, Section 3 details the methodology, Section 4 presents experimental validation, and Section 5 concludes with manufacturing implications and future work.

2. Related Work

2.1. Traditional and AI-Driven Control in R2R Systems

Classical R2R control relies on PID, LQR and MPC variants to regulate web tension and transport speed under strong coupling and changing roll radii. Foundational modeling and robust control for winding systems established today's tension/velocity decoupling strategies [13], while industrial studies refined adaptive PI/PID implementations to cope with operating-point drift [14, 15]. Recent work emphasizes advanced control methods for R2R systems [16, 17], physics-consistent tension models validated on pilot lines [18, 19]. Manufacturing surveys more broadly underline the central role of monitoring and feedback design in achieving product quality and system robustness [20, 21]. Complementing traditional

control design approaches, data-driven R2R studies report robust constrained tension regulation [22] and AI-assisted reconstruction and estimation of tension fields [23, 24], with related web-tension reviews pointing to hybrid controllers as a promising direction [25].

2.2. LLM for Control Design

LLMs increasingly act as planners, code synthesizers, and supervisors for control systems. Agentic frameworks automate various aspects of control design including requirements parsing, loop-shaping, and gain search, then call numerical solvers for verification [26, 27]. In cyber-physical systems, LLM agents co-design objective-oriented controllers and evolve control structures [28, 29]. For safety-critical applications, LLMs translate natural-language specifications into formal artifacts or symbolic-control pipelines [30]. Recent work extends LLM-based control to robust synthesis via linear matrix inequalities (LMI) [31] and adaptive model order reduction for control design [32]. These approaches show promise in automating control design tasks. However, practical deployment in industrial manufacturing remains limited, motivating frameworks that address safety validation.

2.3. LLM in Manufacturing Applications

Manufacturing-focused frameworks position LLMs for data integration, decision support, and workflow automation across processes and shop-floor IT [33, 34]. In production systems, LLM agents have been combined with digital twin resources to aid planning, diagnosis, and human-machine collaboration, while focusing primarily on analytics and high-level decision-making [35, 36, 37]. Studies report LLM-enabled knowledge extraction for process engineering [38], Industrial Internet of Things (IIoT) integration with legacy and smart machines [39], and agentic fault-handling workflows for continuous industries [40]. However, existing manufacturing applications primarily address supervisory control—task sequencing, resource allocation, and fault detection—rather than control design. Prior work focuses on what control actions to take (e.g., which setpoints to command) but not how to design controllers that achieve those setpoints with desired dynamic performance. This gap motivates an LLM-assisted framework for R2R manufacturing that integrates controller design, parameter tuning, and sim-to-real adaptation.

3. Proposed Framework

Integrating LLMs into manufacturing control introduces challenges absent in human operation: ensuring safety despite probabilistic reasoning, maintaining transparent decisions for regulatory compliance, and bridging general-purpose models to domain-specific control expertise. This section presents a framework addressing these through multi-agent collaboration, simulation-based safety validation, and retrieval-augmented domain knowledge integration.

The framework operates through five phases: system initialization (Phase 0), offline controller design (Phase 1), real system deployment (Phase 2), stable operation with monitoring (Phase 3), and periodic model updates (Phase 4). Unlike conventional automation, this implements constrained autonomy—LLMs generate strategies, simulation validates safety, humans retain oversight. Figure 1 shows the closed-loop architecture where operational data informs simulation refinement while LLMs orchestrate design, tuning, and adaptation.

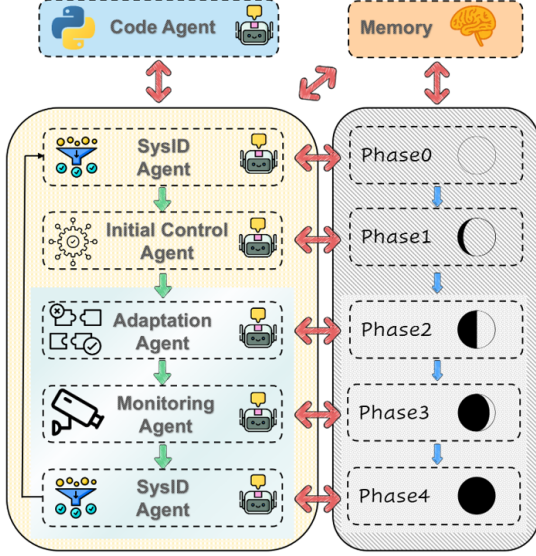


Figure 1: LLM-assisted R2R control framework. All LLM-proposed modifications must pass simulation validation before deployment.

3.1. Multi-Agent Architecture and RAG Integration

The framework’s intelligence emerges from specialized agent collaboration rather than monolithic reasoning. This design addresses a key limitation of applying general-purpose LLMs to control: the need for both broad reasoning capabilities and deep domain expertise at different decision points.

The framework employs five specialized agents with role-specific prompts and domain knowledge access: SysID Agent (system identification), Initial Control Agent (controller tuning and selection), Adaptation Agent (sim-to-real tuning), Monitoring Agent (monitoring and diagnostics), and Code Agent (algorithm application and validated execution). Each interaction is logged with requesting agent, task specification, retrieved knowledge, and validation results.

3.1.1. Prompt Engineering for Control Domain

Control system prompts differ from general LLM applications in four ways: (1) state physical limits clearly to reduce hallucinations, (2) organize reasoning steps from data analysis to testing, (3) mandate validation before deployment, and (4) define protocols for human intervention. As detailed in Appendix A.

3.1.2. RAG for Domain Knowledge Grounding

A major distinction between human engineers and LLMs is knowledge access: humans leverage years of accumulated experience,

while LLMs carry the risk of generating control strategies that appear reasonable yet are dangerous. RAG [8, 39] bridges this gap by dynamically grounding LLM reasoning in verified domain knowledge.

The knowledge base provides 3 hierarchical tiers: (1) control theory fundamentals (stability criteria, design methodologies), (2) R2R best practices (tension control strategies, commissioning procedures), and (3) system-specific documentation (equipment specs, operational history). When agents query, multi-stage retrieval performs semantic embedding, hierarchical search, relevance ranking, and conflict resolution. This enables recall from thousands of documents and consistency verification across sources. Figure 2 illustrates RAG integration for the Initial Control Agent.

3.2. Phase 0: System Identification (SysID Agent)

With the architectural foundation established, we now detail how each phase leverages LLM capabilities. Phase 0 demonstrates how LLMs automate the traditionally expert-driven task of model construction.

This phase constructs a simulation model from operational data and physical principles, serving dual purposes: enabling offline controller design and providing safety filter validation. Figure 3 shows the workflow of SysID Agent.

Historical data $\mathcal{D} = \{(u_k, y_k, t_k)\}_{k=1}^N$ is collected, where $u_k \in \mathbb{R}^m$ represents control inputs, $y_k \in \mathbb{R}^p$ measured outputs, and t_k timestamps. The system dynamics follow a nonlinear state-space representation:

$$\dot{x}(t) = f(x(t), u(t), \theta), \quad y(t) = h(x(t), \theta) \quad (1)$$

where $x(t) \in \mathbb{R}^n$ contains web tensions and roller velocities, θ represents physical parameters, and functions $f(\cdot)$ and $h(\cdot)$ represent the physics of web transport.

The SysID Agent combines data-driven estimation with physics-informed structure. Upon receiving data, it queries RAG for R2R identification practices and analyzes data characteristics to formulate a strategy. The agent automatically translates physical principles into optimization constraints. Rather than relying on a single identification method, the agent implements multiple approaches including recursive least squares, prediction error methods, and subspace identification.

The identification problem minimizes prediction error while regularizing toward prior knowledge from equipment specifications:

$$\theta^* = \arg \min_{\theta} \sum_{k=1}^N \|y_k - \hat{y}_k(\theta)\|_2^2 + \lambda \|\theta - \theta_{\text{prior}}\|_2^2 \quad (2)$$

The regularization term prevents overfitting and constrains parameters to physically meaningful ranges.

The control objective is defined as:

$$\min_{u(t)} J = \int_0^{T_f} [Q(y(t) - y_{\text{ref}}(t))^2 + Ru(t)^2] dt \quad (3)$$

subject to physical and operational constraints:

$$x_{\min} \leq x(t) \leq x_{\max}, \quad u_{\min} \leq u(t) \leq u_{\max} \quad (4)$$

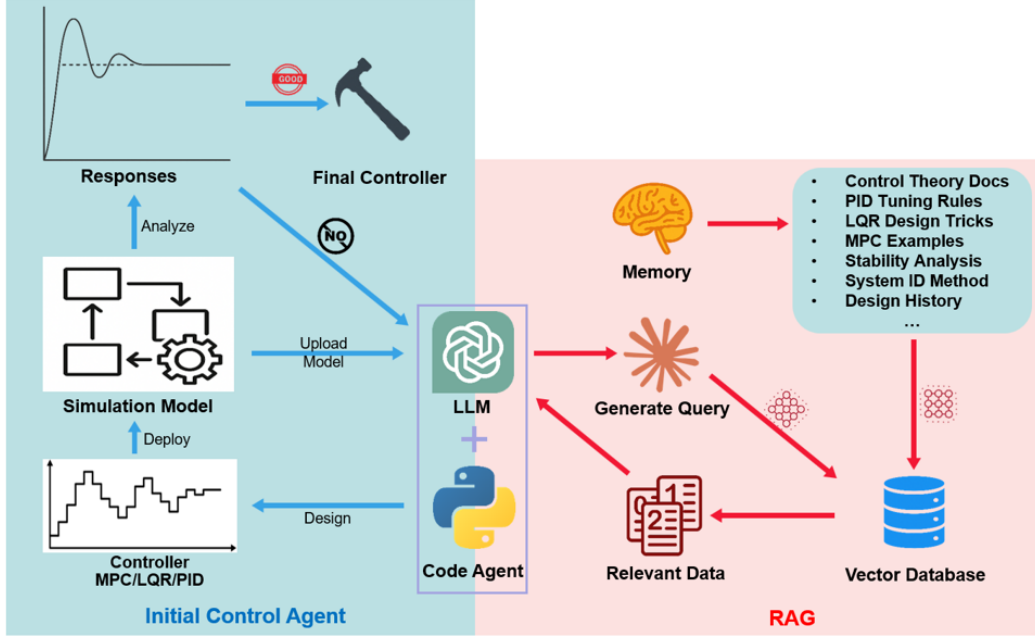


Figure 2: Initial Control Agent with RAG integration. All agents access this infrastructure; detailed here for clarity.

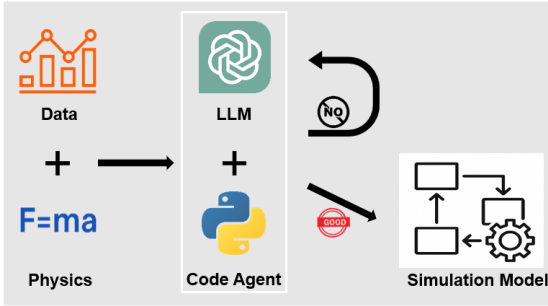


Figure 3: SysID Agent workflow

where Q and R are weighting matrices, and $y_{\text{ref}}(t)$ is the reference trajectory.

3.3. Phase 1: Controller Design and Selection (Initial Control Agent)

Building on the validated model, this phase evaluates three architectures. The LLM first analyzes system characteristics such as tension-velocity coupling strength and dynamic time scales to match appropriate controller architectures. This includes determining whether to linearize the nonlinear dynamics around operating points for controllers like LQR, or to use the full nonlinear model for nonlinear control approaches. It then reasons about parameter spaces using control theory principles to guide the tuning process. Finally, it evaluates trade-offs between competing objectives—tracking accuracy, settling speed, energy consumption, and robustness.

The PID controller is implemented as:

$$u(t) = K_p e(t) + K_i \int_0^t e(\tau) d\tau + K_d \frac{de(t)}{dt} \quad (5)$$

where $e(t) = y_{\text{ref}}(t) - y(t)$ is the tracking error, and K_p , K_i , K_d are the proportional, integral, and derivative gains.

The MPC optimization problem at time step k is formulated as:

$$\min_{\mathbf{u}} \sum_{i=0}^{N_p-1} \left[\|\mathbf{y}(k+i|k) - \mathbf{y}_{\text{ref}}(k+i)\|_Q^2 + \|\mathbf{u}(k+i)\|_R^2 \right] \quad (6)$$

subject to system dynamics and constraints over prediction horizon N_p .

For the linearized system $\dot{x} = Ax + Bu$, the LQR control law is:

$$u(t) = -Kx(t), \quad K = R^{-1}B^T P \quad (7)$$

where P solves the continuous-time algebraic Riccati equation:

$$A^T P + PA - PBR^{-1}B^T P + Q = 0 \quad (8)$$

For each controller architecture, the LLM employs iterative reasoning to tune hyperparameters $\phi = \{K_p, K_i, K_d\}$ for PID, or equivalent parameters for MPC and LQR. The tuning process is described in Algorithm 1, where the LLM analyzes simulation responses and adjusts parameters to optimize the control objective defined in Equation (3).

Performance metrics evaluated include root mean square error quantifying tracking accuracy:

$$e_{\text{RMSE}} = \sqrt{\frac{1}{N} \sum_{k=1}^N (y_k - y_{\text{ref},k})^2} \quad (9)$$

Settling time measuring speed of convergence to steady-state:

$$t_s = \min\{t : |y(\tau) - y_{\infty}| \leq 0.02|y_{\infty}|, \forall \tau \geq t\} \quad (10)$$

Algorithm 1 Initial Control Agent

Require: Simulation model S_{sim} , controller type C , objective J

Ensure: Optimized hyperparameters ϕ^*

- 1: LLM retrieves tuning guidelines from RAG, initializes ϕ_0
- 2: $i \leftarrow 0$, max_iterations $\leftarrow 50$
- 3: **while** $i < \text{max_iterations}$ AND not converged **do**
- 4: Code Agent: Execute simulation with $C(\phi_i)$, compute $P(t)$
- 5: LLM: Diagnose limitations, query RAG, generate ϕ_{i+1} with justification
- 6: Validate stability and constraints
- 7: **if** $J(\phi_{i+1}) < J(\phi_i)$ AND validated **then**
- 8: Accept ϕ_{i+1} , log reasoning
- 9: **else**
- 10: LLM revises strategy
- 11: **end if**
- 12: $i \leftarrow i + 1$
- 13: **end while**
- 14:
- 15: **return** ϕ^* with tuning history

Overshoot percentage indicating stability margin and oscillatory behavior:

$$OS = \frac{\max(y(t)) - y_{\infty}}{y_{\infty}} \times 100\% \quad (11)$$

Control effort measuring energy consumption and actuator stress:

$$U_{\text{total}} = \int_0^{T_f} u(t)^2 dt \quad (12)$$

Robustness quantifying worst-case performance under model uncertainty:

$$\mathcal{R} = \max_{\|\Delta\theta\| \leq \epsilon} \|y(t; \theta + \Delta\theta) - y(t; \theta)\|_{\infty} \quad (13)$$

Define the performance vector as $P(t) = [e_{\text{RMSE}}(t), OS(t), t_s(t)]^T$, characterizes controller performance across accuracy, speed, stability, efficiency, and robustness dimensions.

Selection via weighted score balancing multiple objectives:

$$S = w_1 e_{\text{RMSE}} + w_2 t_s + w_3 OS + w_4 U_{\text{total}} + w_5 \mathcal{R} + w_6 C_{\text{comp}} \quad (14)$$

where weights w_i reflect manufacturing priorities and C_{comp} accounts for computational feasibility.

$$C^* = \arg \min_{C \in \{\text{PID}, \text{MPC}, \text{LQR}\}} S(C) \quad (15)$$

This optimal controller C^* with its tuned parameters ϕ^* is then prepared for deployment to the real system in Phase 2.

3.4. Phase 2: Sim-to-Real Adaptation (Adaptation Agent)

Phase 2 addresses sim-to-real gap through iterative adaptation, which is constrained autonomy: LLM proposes modifica-

tions, but every change must pass safety validation. Figure 4 shows the workflow.

3.4.1. Safety Filter

A fundamental challenge is that LLMs generate probabilistic suggestions without safety guarantees. Human engineers rely on physical intuition to avoid dangerous choices; LLMs lack this. Our safety filter implements mandatory pre-validation: every proposed modification must demonstrate safe operation in simulation before hardware deployment.

The filter evaluates three criteria. Constraint satisfaction verifies all operational limits are maintained throughout the control horizon:

$$C_{\text{safe}} = \begin{cases} u_{\min} \leq u_i(t) \leq u_{\max}, & \forall i, t \\ |\dot{u}_i(t)| \leq \dot{u}_{\max}, & \forall i, t \end{cases} \quad (16)$$

where the rate constraint on control derivatives prevents actuator damage from abrupt torque changes that could occur with aggressive LLM-suggested parameters.

Performance improvement ensures modifications enhance rather than degrade tracking accuracy, settling behavior, and overshoot:

$$\mathcal{P}_{\text{improved}} = \|P_{\text{proposed}}(t)\|_2 < \|P_{\text{current}}(t)\|_2 \quad (17)$$

This metric prevents the LLM from suggesting changes that satisfy constraints but worsen control quality—a scenario human operators would recognize but requires explicit verification for LLMs.

Stability margins assess robustness through worst-case performance under parametric uncertainty:

$$\mathcal{S}_{\text{robust}} = \max_{\|\Delta\theta\| \leq \epsilon} \|y(t; \theta + \Delta\theta) - y_{\text{ref}}(t)\|_{\infty} < \delta_{\text{tol}} \quad (18)$$

Robustness is important because simulation models inevitably contain uncertainty; controllers must maintain stability despite model mismatch.

Deployment approval requires all three criteria to be satisfied simultaneously:

$$\text{Approve} = C_{\text{safe}} \wedge \mathcal{P}_{\text{improved}} \wedge \mathcal{S}_{\text{robust}} \quad (19)$$

providing a safety barrier between LLM suggestions and physical implementation.

Safety filter provides capabilities difficult for humans: testing across comprehensive scenarios in seconds, zero fatigue across iterations, quantitative stability margins versus qualitative assessment, and automatic rollback preparation.

3.4.2. Adaptation Process

The adaptation process (Algorithm 2) implements structured iteration that begins with deploying the Phase 1 controller $C^*(\phi^*)$ to the real system. The Adaptation Agent then analyzes the performance gap between simulation and reality to diagnose the root cause of mismatch. Based on this diagnosis, it proposes parameter adjustments that must pass the simulation safety filter before deployment to hardware. This cycle repeats until the controller meets the convergence criteria defined in Equation (20).

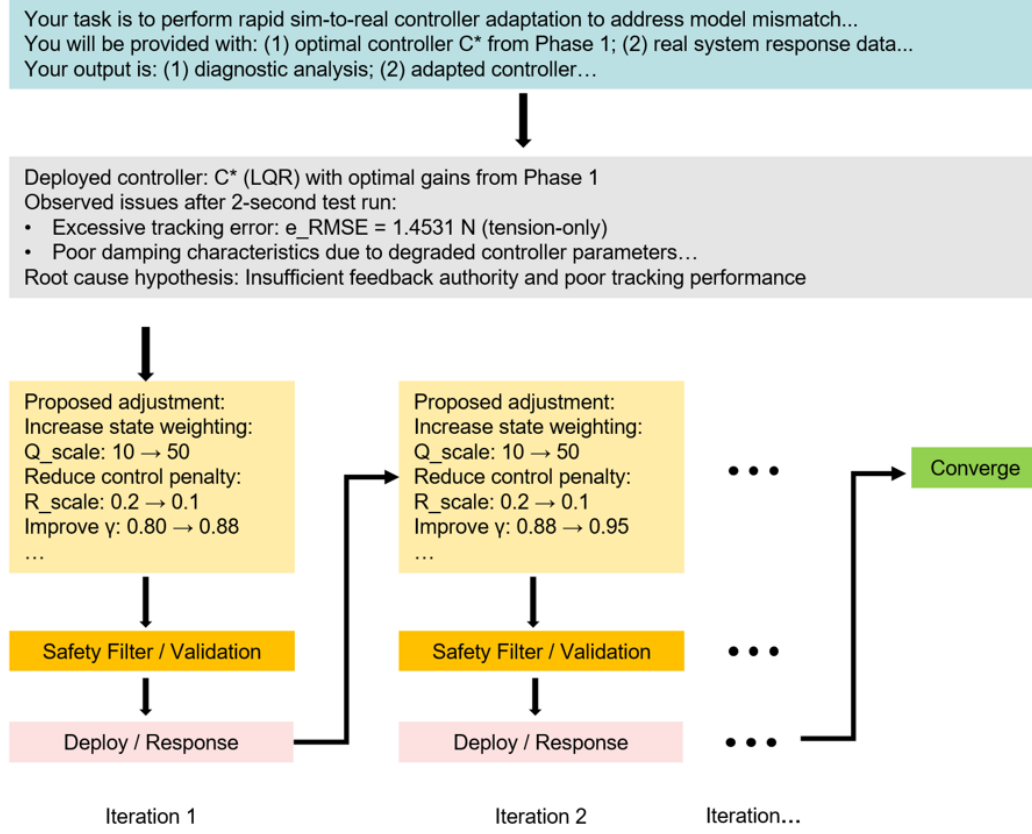


Figure 4: Adaptation Agent with mandatory safety filter. Simulation-in-the-loop ensures zero unsafe deployments.

Algorithm 2 Adaptation Agent

Require: Controller $C^*(\phi^*)$, real system S_{real} , thresholds, simulation S_{sim}

Ensure: Adapted controller C_{adapted}

- 1: Deploy $C^*(\phi^*)$ to S_{real}
- 2: iteration $\leftarrow 0$
- 3: **repeat**
- 4: Monitor tension $T(t)$ and velocity $v(t)$, compute $P_{\text{real}}(t)$
- 5: **if** $P_{\text{real}}(t)$ satisfies Eq. (20) **then**
- 6: Performance met, exit
- 7: **end if**
- 8: LLM: Analyze gap ΔP , query RAG for causes, diagnose root cause
- 9: LLM: Generate $\Delta\phi$ with justification
- 10: Safety Filter: Test $C(\phi + \Delta\phi)$ in S_{sim}
- 11: Verify per Eqs. (16)–(18)
- 12: **if** approved per Eq. (19) **then**
- 13: Deploy $\phi \leftarrow \phi + \Delta\phi$ to S_{real}
- 14: Log: parameters, reasoning, results
- 15: **else**
- 16: Reject, LLM revises
- 17: **end if**
- 18: iteration \leftarrow iteration + 1
- 19: **until** converged OR max iterations
- 20:
- 21: **return** C_{adapted} with history

Convergence criteria define when real system performance meets production requirements:

$$P_{\text{real}}(t) < P_{\text{threshold}} = [0.05 \cdot T_{\text{ref}}, 20\%, 2.0s]^T. \quad (20)$$

3.5. Phase 3: Intelligent Monitoring (Monitoring Agent)

Following successful adaptation, Phase 3 implements continuous monitoring with autonomous diagnostics. Unlike threshold-based alarms, the agent performs dual-layer analysis: detecting degradation and diagnosing root causes—distinguishing control-adjustable issues from physical maintenance needs. Figure 5 shows the architecture.

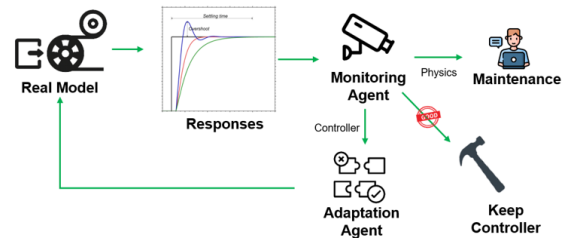


Figure 5: Monitoring Agent dual-layer architecture

LLM capabilities beyond human monitoring: (1) 24/7 vigilance without fatigue, (2) multi-hypothesis reasoning with confidence scores avoiding cognitive bias, (3) cross-domain knowledge integration from RAG.

Layer 1 detects degradation by computing the Euclidean distance from baseline performance:

$$\Delta P(t) = \|P(t) - P_{\text{baseline}}\|_2 > 2\sigma_{\text{baseline}} \quad (21)$$

using a statistical threshold that adapts to normal process variability captured in σ_{baseline} .

Layer 2 diagnoses causes: material property variations, mechanical degradation (bearing wear, belt slippage), sensor issues (drift, noise), environmental factors, or process disturbances. The agent formulates hypotheses by matching observed patterns against RAG-retrieved failure modes, assigning confidence based on evidence strength:

$$H_j = \{\text{hypothesis}_j, \text{confidence}_j, \text{evidence}_j, \text{action}_j\} \quad (22)$$

Algorithm 3 Monitoring Agent

Require: Real-time data stream $\mathcal{D}_{\text{live}}$, baseline performance P_{baseline}

Ensure: Adapted controller or maintenance alert

- 1: Monitor $P(t)$ continuously
 - 2: **if** degradation detected per Eq. (21) **then**
 - 3: Route to Adaptation Agent for control adaptation
 - 4: **if** adaptation successful: performance recovers to $\Delta P < \sigma_{\text{baseline}}$ **then**
 - 5: Deploy adapted controller
 - 6: Perform Layer 2 diagnostics to identify root cause
 - 7: Log findings for predictive maintenance
 - 8: **else**
 - 9: Send immediate maintenance alert
 - 10: Perform Layer 2 diagnostics for root cause analysis
 - 11: Provide diagnostic evidence to maintenance team
 - 12: Continue with current controller pending repair
 - 13: **end if**
 - 14: **end if**
-

3.6. Phase 4: Continuous Model Refinement (SysID Agent)

During scheduled R2R system downtime or rest periods, accumulated operational data $\mathcal{D}_{\text{ops}} = \{(u_k, y_k, t_k)\}_{k=1}^M$ from Phases 2 and 3 is used to refine the simulation model. The simulation model parameters are re-identified following the same system identification and physics-informed construction procedures established in Phase 0, ensuring the simulation environment remains representative of the evolving real system dynamics and safety validation remains representative. Simultaneously, the controller parameters ϕ_{stable} that achieved stable operation in Phase 3 are archived as the validated baseline configuration. For subsequent production runs, these archived controller parameters can be deployed directly to the real system.

4. Experimental Validation

This section validates the proposed LLM-assisted control framework through a simulation study of a R2R web handling system.

4.1. System Description and Dynamic Model Formulation

The first validation employs a multi-span R2R web handling system representative of industrial processes such as printing and coating. The system schematic and nomenclature are shown in Figure 6. Following established approaches [41, 42], the model adopts three key assumptions: (1) Passive rollers are neglected, with only actuated motorized rollers considered [42]. (2) Web tension T_i remains uniform within each span i between adjacent rollers. (3) The no-slip condition $v_i = \omega_i R_i$ holds due to sufficiently high friction.

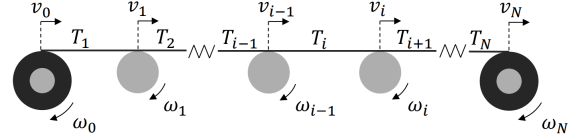


Figure 6: Schematic of a simplified R2R line

The system dynamics couple web tension evolution and roller velocity through differential equations. Web tension dynamics in span i follow the viscoelastic relation [41]:

$$\frac{dT_i}{dt} = \frac{AE}{L_i}(v_i - v_{i-1}) + \frac{1}{L_i}(T_{i-1}v_{i-1} - T_i v_i) \quad (23)$$

where A is web cross-sectional area, E is elastic modulus, L_i is span length, and v_i, v_{i-1} are roller velocities. Roller velocity dynamics from torque balance are:

$$\frac{dv_i}{dt} = \frac{R_i^2}{J_i}(T_{i+1} - T_i) - \frac{f_i}{J_i}v_i + \frac{R_i}{J_i}u_i + b_i\xi_i(t) \quad (24)$$

where R_i is roller radius, J_i is moment of inertia, f_i is viscous friction, u_i is control torque, and $b_i\xi_i(t)$ captures stochastic disturbances. Parameters $\theta = \{E, A, L_i, R_i, J_i, f_i\}$ are identified following Phase 0 procedures. The validation uses three parameter sets: real system $\mathcal{S}_{\text{real}}$ generating operational data, identified model $\mathcal{S}_{\text{real,ID}}$ from Phase 0 system identification with 1.4-8.6% estimation errors, and intentionally mismatched simulation model \mathcal{S}_{sim} with 8.3-50% deviations to test adaptation robustness under significant sim-to-real gap (Table 1). This conservative setting ensures generalizability—by testing under intentionally large model mismatches, successful adaptation here suggests the framework should perform well in typical real-world scenarios where gaps are smaller.

Table 1: System Parameters: Real, Identified, and Simulation Models

Symbol (Unit)	$\mathcal{S}_{\text{real}}$	$\mathcal{S}_{\text{real,ID}}$	\mathcal{S}_{sim}
EA (N)	2200	2169.85	2400
J (kg·m ²)	1.0	1.078	0.95
R (m)	0.035	0.038	0.04
f_i (N·m·s/rad)	15.0	15.47	10.0
L (m)	1.2	1.24	1.0
Disturbance coefficient (s·m ⁻¹ ·kg ⁻¹)	$5 \cdot 10^{-2}$	-	10^{-2}
Number of spans	6	6	6

4.2. Tension control

Experimental Configuration. The tension control scenario maintains setpoints $T_1 = 28$ N, $T_2 = 36$ N, $T_4 = 40$ N, $T_5 = 24$ N, and $T_6 = 32$ N, with web 3 executing a step change from 20 N to 44 N at $t = 1$ s to simulate process disturbances. Unwinding velocity is $v_0 = 0.01$ m/s, with reference roller velocities computed as:

$$v_i^r(t) = \frac{EA - T_{i-1}(t)}{EA - T_i(t)} v_{i-1}^r(t), \quad v_0^r = v_0 \quad (25)$$

Controller Adaptation. The Initial Control Design Agent selected LQR based on Table 2. Figure 7 and Figure 8 show three sequential adaptation phases. Initial controller has large tracking errors and control oscillations upon initial deployment. While Adapt1,2 demonstrates improved stability with smooth control inputs.

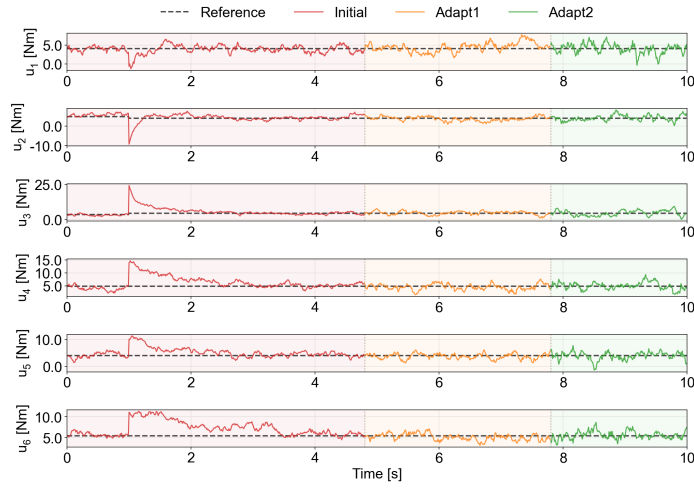


Figure 7: Control input trajectories during tension control

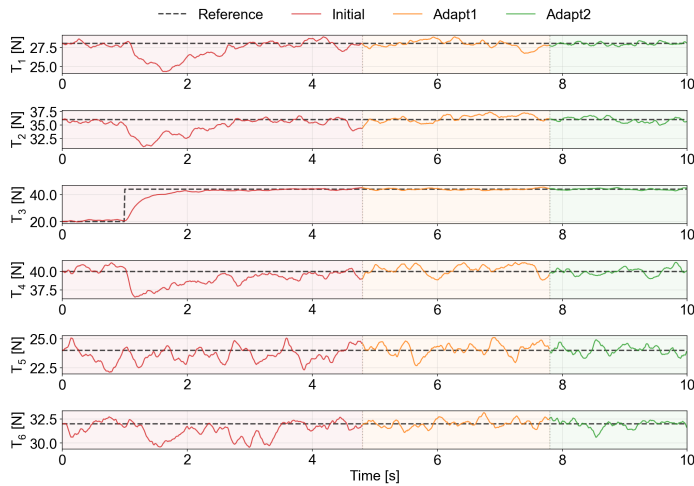


Figure 8: Tension trajectories during tension control

Performance Comparison Under Identical Conditions. Figure 9 compares controllers Initial-Adapt2 under identical conditions to isolate performance improvements. Initial exhibits sus-

tained errors exceeding 3 N in spans T_1 , T_2 , T_4 , and T_5 , while Adapt2 achieve tracking within ± 1 N.

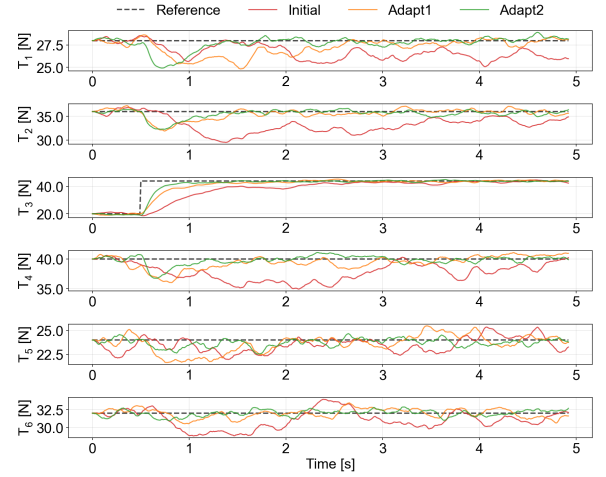


Figure 9: Comparative tension tracking performance across three adaptation cycles under identical conditions

4.3. Change in velocity setpoint

Experimental Configuration. The velocity tracking scenario evaluates controller robustness during process acceleration transients common in R2R manufacturing startup and grade change operations. All six web spans maintain constant reference tensions at $T_i = 30$ N throughout the experiment. The unwinding velocity executes a step increase from $v_0 = 0.01$ m/s to $v_0 = 0.10$ m/s at $t = 1$ s, representing a 10-fold acceleration. Reference roller velocities for all actuated rollers are computed according to Equation (25) to maintain equilibrium tension distribution during the velocity transient.

Controller Adaptation. The same LQR controller selected in the tension control scenario was deployed for velocity tracking validation. Figure 10 and Figure 11 present control inputs and tension trajectories during sequential adaptation. Initial exhibits poor tension regulation during and after the velocity ramp, with multiple spans showing oscillatory behavior and deviations from the 30 N setpoint. The Adaptation Agent identified insufficient feedforward compensation during velocity transients and excessive feedback gains causing post-transient oscillations. The suggested parameter adjustments, validated through simulation safety filter, were deployed as Adapt1, demonstrating reduced oscillations but persistent steady-state errors in several spans. Adapt2 achieves improved regulation with tensions remaining closer to reference during the acceleration phase and subsequent steady-state operation.

Performance Comparison Under Identical Conditions. Figure 12 compares the initial controller Initial with three sequentially adapted versions (Adapt1, Adapt2, Adapt3) under identical velocity ramping conditions. Initial shows sustained tension deviations exceeding 4 N in spans T_1 , T_2 , T_3 , and T_5 during both transient and steady-state phases. Adapt1 reduces transient deviations substantially, while Adapt2 and Adapt3 main-

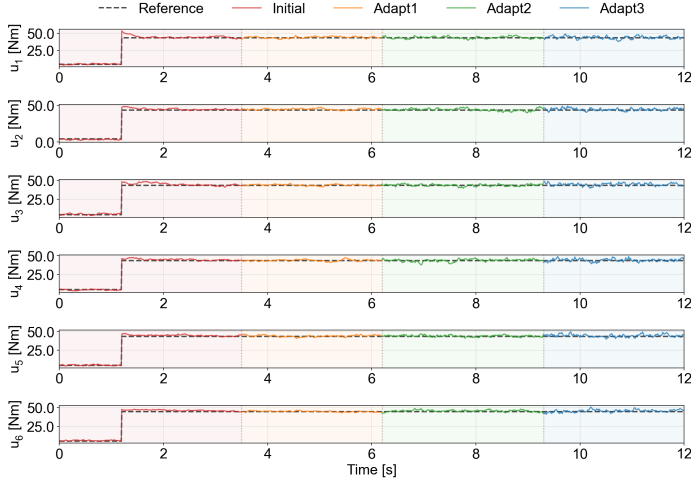


Figure 10: Control input trajectories during velocity setpoint change

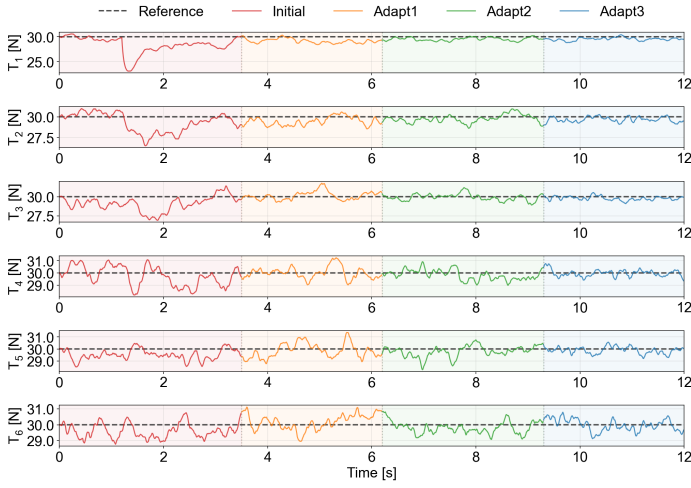


Figure 11: Tension trajectories during velocity setpoint change

tain tensions within ± 1 N throughout the acceleration and post-transient periods.

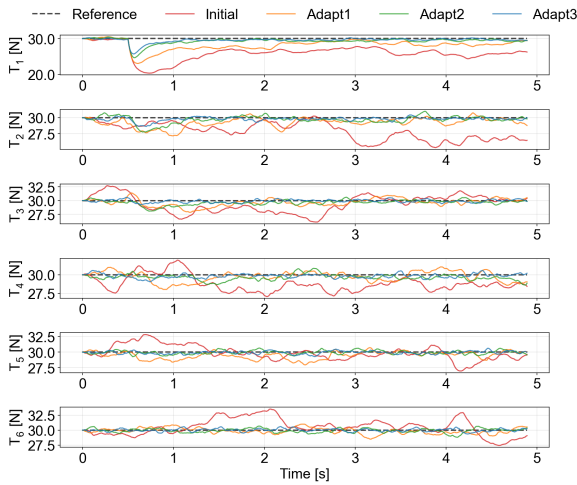


Figure 12: Comparative tension regulation performance during velocity ramping across four adaptation cycles under identical conditions

4.4. Detailed Agent Interactions

This subsection demonstrates the practical implementation of the LLM-assisted framework through the tension control scenario with setpoints $T_1 = 28$ N, $T_2 = 36$ N, T_3 step change from 20 N to 44 N at $t = 1$ s, $T_4 = 40$ N, $T_5 = 24$ N, and $T_6 = 32$ N. All agents follow system prompts defined in Section [Appendix A](#), with the complete workflow shown in Figure 13.

Phase 0: System Identification. The SysID Agent queries RAG (all agents have access to RAG for domain knowledge retrieval; for brevity, RAG interaction is shown explicitly only for the SysID Agent) for physics-informed identification best practices, then directs the Code Agent to implement constrained optimization with recursive least squares. The Code Agent generates a Python implementation using `scipy.optimize` and executes parameter identification on historical data points. Results yield parameter vector θ . The validated simulation model \mathcal{S}_{sim} is stored in Model Repository.

Phase 1: Controller Design. The Initial Control Agent systematically evaluates three controller architectures through simulation, with comparative performance metrics presented in Table 2. Each controller is tuned following Algorithm 1 through iterative Code Agent implementation and testing. Based on comprehensive evaluation, the agent selects LQR as C^* .

Table 2: Comparative Performance of Controller Architectures in Simulation Environment

Type	e_{RMSE} (N)	t_s (s)	OS (%)	U_{total}	C_{comp} (ms)
PID	0.4813	1.05	16.41	706.20	0.0082
MPC	0.5843	1.18	13.89	703.64	0.2319
LQR	0.3811	1.62	16.31	703.81	0.0002

Phase 2: Sim-to-Real Adaptation. A continuous 10-second simulation validates iterative adaptation with controller parameter switches at $t = 4.8$ s and $t = 7.8$ s. Initial deployment uses: $Q_{scale} = 10$, $R_{scale} = 0.2$, $c_I = 0.1$, $\gamma = 0.80$, resulting in poor performance with $e_{RMSE} = 1.0275$ N and tension RMSE = 1.4531 N. The Adaptation Agent analyzes response data and directs the Code Agent to test adjusted parameters in simulation safety filter: increase state weighting ($Q_{scale} : 10 \rightarrow 50$), reduce control penalty ($R_{scale} : 0.2 \rightarrow 0.1$), strengthen integral action ($c_I : 0.1 \rightarrow 0.2$), and improve persistence ($\gamma : 0.80 \rightarrow 0.88$). The Code Agent validates Adapt1 candidate. Adapt1 deploys at $t = 4.8$ s with $e_{RMSE} = 0.4973$ N. The agent identifies remaining 24.1% performance gap and proposes further refinement. After Code Agent validation through safety filter, Adapt2 deploys at $t = 7.8$ s, achieving convergence.

Phase 3: Continuous Monitoring. To validate Phase 3 monitoring capabilities, friction is increased from $f_i = 15.0$ to $f_i = 30.0$ N-m-s/rad at $t = 72$ hours, simulating severe mechanical wear. The Monitoring Agent detects degradation and routes the issue to the Adaptation Agent, which successfully recovers performance through a single adaptation iteration, as shown in Figure 14. Subsequent Layer 2 diagnostics identify friction

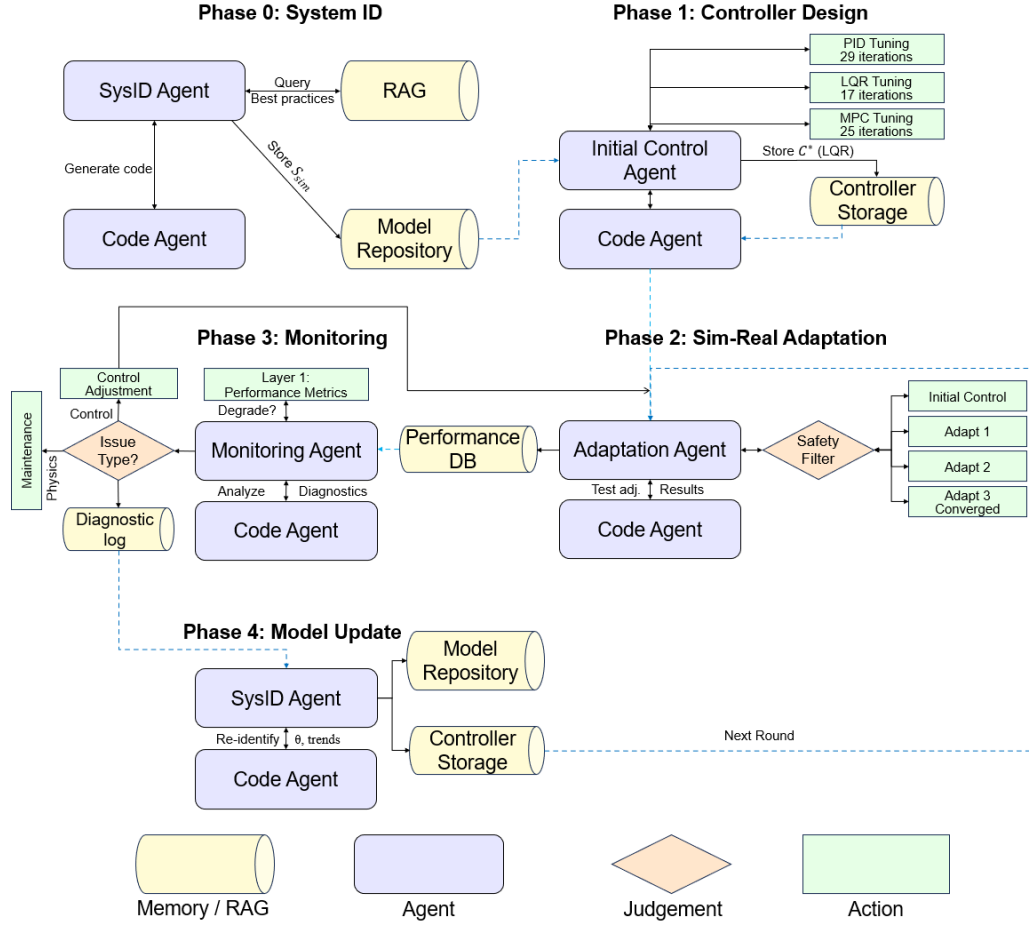


Figure 13: Detailed workflow of Adaptation Agent

degradation (72% confidence), encoder degradation introducing measurement noise (68% confidence), bearing wear increasing effective inertia J (63% confidence), and belt/coupling wear adding mechanical compliance (59% confidence), with the complete diagnostic report logged for predictive maintenance planning.

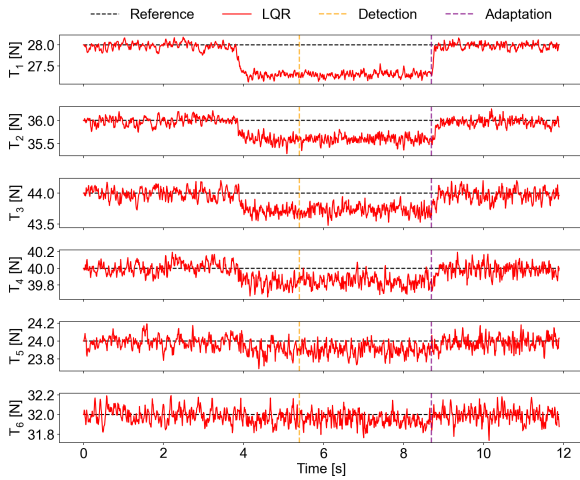


Figure 14: Detection and adaptation for friction change

Phase 4: Model Refinement. Following the complete operational cycle, the SysID Agent re-identifies system parameters using accumulated operational data, successfully capturing the degraded friction state: $f_i = 34.85$ N·m·s/rad (ground truth: 30.0), $J = 1.12$ kg·m², $R = 0.0312$ m, $L = 1.23$ m, $EA = 2139.39$ N. The updated model S_{sim} with refined parameters enables improved controller design for subsequent production runs.

5. Conclusion and Future Work

This work presents an LLM-assisted multi-agent control framework that integrates LLM with controller design for R2R manufacturing systems. The framework explores sim-to-real adaptation through simulation-validated tuning, working toward stable tension control and velocity tracking despite major model mismatch. Experimental validation shows controller selection, iterative adaptation, and monitoring with diagnostic capabilities.

Future work will focus on: (1) hardware validation on physical R2R testbeds; (2) extension to other manufacturing processes beyond R2R systems; and (3) development of transfer learning strategies to accelerate deployment across different R2R configurations.

Acknowledgements

This work is based upon work partially supported by the National Science Foundation under Cooperative Agreement No. CMMI-2041470. Any opinions, findings and conclusions expressed in this material are those of the author(s) and do not necessarily reflect the views of the National Science Foundation.

Appendix A. Detailed Prompt for Each Agent

This section provides the complete system prompts that define the role, inputs, and expected outputs for each specialized agent in the framework.

A.1. SysID Agent System Prompt

Agent Role: System Identification Expert

Your task: Construct a physics-informed simulation model of the R2R manufacturing system through systematic parameter identification.

Inputs provided: (1) Historical operational data containing control inputs u_k , measured outputs y_k (tensions and velocities), and timestamps t_k ; (2) System dynamic equations (Equations (23) and (24)); (3) RAG access to domain knowledge on R2R system identification best practices; (4) Physical parameter bounds and constraints.

Required outputs: (1) Identified parameter vector θ with confidence intervals; (2) Validation metrics (R^2 scores for tension and velocity predictions, mean absolute errors); (3) Constructed simulation model \mathcal{S}_{sim} stored in System Model Repository; (4) Assessment of model fidelity and recommendations for controller design phase.

A.2. Initial Control Agent System Prompt

Agent Role: Controller Design and Selection Expert

Your task: Design, compare, and select the optimal controller architecture for the R2R tension control system through systematic simulation-based evaluation.

Inputs provided: (1) Validated simulation model \mathcal{S}_{sim} from Phase 0; (2) Control objectives and constraints (Equations (3), (4)); (3) Three candidate controller architectures (PID, MPC, LQR) with their mathematical formulations (Equations (5), (6), (7)); (4) Performance metrics for evaluation (Equations (9) through (13)); (5) Code Agent for implementation and testing.

Required outputs: (1) Tuned hyperparameters for each controller architecture following Algorithm 1; (2) Comparative performance table with all metrics; (3) Selection decision with detailed engineering justification; (4) Optimal controller C^* with configuration stored in Controller Configuration Storage for Phase 2 deployment.

A.3. Adaptation Agent System Prompt

Agent Role: Sim-to-Real Adaptation Specialist

Your task: Perform rapid sim-to-real controller adaptation to address model mismatch between simulation and physical hardware through iterative tuning validated by simulation safety filter.

Inputs provided: (1) Optimal controller C^* with parameters ϕ^* from Phase 1; (2) Real system response data from deployment tests; (3) Simulation model \mathcal{S}_{sim} for safety validation; (4) Performance convergence criteria (Equation (20)); (5) Code Agent for testing adjustments.

Required outputs: (1) Diagnostic analysis identifying specific model mismatch symptoms and root causes; (2) Suggested parameter adjustments $\Delta\phi$ with control-theoretic justification; (3) Simulation safety filter validation results per Equation (19); (4) Adapted controller parameters ϕ_{final} when convergence criteria satisfied; (5) Complete adaptation history stored in Performance Baseline Database.

Design process: Follow Algorithm 2 for structured iteration.

A.4. Monitoring Agent System Prompt

Agent Role: Performance Monitoring and Diagnostics Expert

Your task: Perform continuous dual-layer performance monitoring and diagnostic analysis during stable production operation to detect degradation and distinguish between control-adjustable issues and physical maintenance requirements.

Inputs provided: (1) Real-time operational data stream \mathcal{D}_{live} containing tensions, velocities, and control signals; (2) Baseline performance vector $P_{baseline}$ established at Phase 2 completion; (3) Degradation detection threshold per Equation (21); (4) Simulation model \mathcal{S}_{sim} for validating adaptive adjustments; (5) Code Agent for implementing diagnostic algorithms.

Required outputs: (1) **Layer 1 analysis**—Continuous performance metric evaluation $\Delta P(t)$ with degradation flags; (2) **Layer 2 analysis**—Root cause diagnostics when degradation detected, categorizing issues as material property variations, mechanical degradation, sensor problems, environmental factors, or process disturbances; (3) Diagnostic reports with confidence-weighted hypotheses distinguishing control vs. maintenance issues; (4) For control-related issues: suggested parameter adjustments validated through simulation safety filter; (5) For physical issues: maintenance alerts with detailed evidence and recommended actions; (6) Adaptation history logged in Diagnostic History Log.

Design process: Follow Algorithm 3 for structured response protocol.

References

- [1] Greener, J., Pearson, G., Cakmak, M., 2018. Roll-to-roll manufacturing: process elements and recent advances. John Wiley & Sons.
- [2] Yan, J., Du, X., 2020. Web tension and speed control in roll-to-roll systems. In: **Control Theory in Engineering**. IntechOpen, p. 209.
- [3] Brandenburg, G., 1976. New mathematical models for web tension and register error. In: 3rd International IFAC Conference on Instrumentation and Automation in the Paper, Rubber and Plastics Industries, vol. 1.
- [4] Saad, G., 2000. Multivariable control of web processes. PhD thesis.
- [5] Niu, S.S., Xiao, D., 2022. Process control: engineering analyses and best practices. Springer Nature.
- [6] Wang, L., Ma, C., Feng, X., Zhang, Z., Yang, H., Zhang, J., Chen, Z., Tang, J., Chen, X., Lin, Y., et al., 2024. A survey on large language model based autonomous agents. *Frontiers of Computer Science* 18(6), 186345.
- [7] Lewis, P., Perez, E., Piktus, A., Petroni, F., Karpukhin, V., Goyal, N., Küttler, H., Lewis, M., Yih, W.T., Rocktäschel, T., et al., 2020. Retrieval-augmented generation for knowledge-intensive nlp tasks. *Advances in Neural Information Processing Systems* 33, 9459–9474.
- [8] Gao, Y., Xiong, Y., Gao, X., Jia, K., Pan, J., Bi, Y., Dai, Y., Sun, J., Wang, H., 2023. Retrieval-augmented generation for large language models: A survey. *arXiv preprint arXiv:2312.10997*.
- [9] Kirchner, S., Knoll, A.C., 2025. Generating automotive code: Large language models for software development and verification in safety-critical systems. *arXiv preprint arXiv:2506.04038*.
- [10] Samak, T.V., Samak, C.V., Li, B., Krovci, V., 2025. When digital twins meet large language models: realistic, interactive, and editable simulation for autonomous driving. *arXiv preprint arXiv:2507.00319*.
- [11] Brintrup, A., Baryannis, G., Tiwari, A., Ratchev, S., Martinez-Arellano, G., Singh, J., 2023. Trustworthy, responsible, ethical AI in manufacturing and supply chains: synthesis and emerging research questions. *arXiv preprint arXiv:2305.11581*.
- [12] Baptista, M.L., Yue, N., Islam, M.M.M., Prendinger, H., 2025. Large Language Models (LLMs) for Smart Manufacturing and Industry X.0. In: **Artificial Intelligence for Smart Manufacturing and Industry X.0**. Springer, pp. 97–119.
- [13] Koc, H., Knittel, D., De Mathelin, M., Abba, G., 2002. Modeling and robust control of winding systems for elastic webs. *IEEE Transactions on Control Systems Technology* 10(2), 197–208.
- [14] Raul, P.R., Pagilla, P.R., 2015. Design and implementation of adaptive PI control schemes for web tension control in roll-to-roll (R2R) manufacturing. *ISA Transactions* 56, 276–287.
- [15] Chen, Q., Li, W., Chen, G., 2016. FUZZY P+ ID controller for a constant tension winch in a cable laying system. *IEEE Transactions on Industrial Electronics* 64(4), 2924–2932.
- [16] Martin, C., Li, W., Chen, D., 2024. Stabilization of almost periodic piecewise linear systems with norm-bounded uncertainty for roll-to-roll dry transfer manufacturing processes. In: 2024 American Control Conference (ACC), pp. 1121–1126.
- [17] Martin, C., Li, W., Chen, D., 2025. Sequential quadratic programming iterative learning control for a roll-to-roll manufacturing process. *ASME Letters in Dynamic Systems and Control* 5(4), 041007.
- [18] Jeong, J., Gafurov, A.N., Park, P., Kim, I., Kim, H.-C., Kang, D., Oh, D., Lee, T.-M., 2021. Tension modeling and precise tension control of roll-to-roll system for flexible electronics. *Flexible and Printed Electronics* 6(1), 015005.
- [19] He, K., Li, S., He, P., Li, J., Wei, X., 2024. Multi-Span Tension Control for Printing Systems in Gravure Printed Electronic Equipment. *Applied Sciences* 14(18), 8483.
- [20] Martin, C., Zhao, Q., Bakshi, S., Chen, D., Li, W., 2022. H_∞ optimal control for maintaining the R2R peeling front. *IFAC-PapersOnLine* 55(37), 663–668.
- [21] Martin, C., Kim, E., Velasquez, E., Li, W., Chen, D., 2025. H_∞ performance analysis for almost periodic piecewise linear systems with application to roll-to-roll manufacturing control. *arXiv preprint arXiv:2508.21199*.
- [22] Chen, Z., Qu, B., Jiang, B., Forrest, S.R., Ni, J., 2023. Robust constrained tension control for high-precision roll-to-roll processes. *ISA Transactions* 136, 651–662.
- [23] Gafurov, A.N., Kim, J., Kim, I., Lee, T.-M., 2025. Web tension AI modeling and reconstruction for digital twin of roll-to-roll system. *Journal of Intelligent Manufacturing* 36(7), 4977–4995.
- [24] Gafurov, A.N., Lee, S., Ali, U., Irfan, M., Kim, I., Lee, T.-M., 2025. AI-driven digital twin for autonomous web tension control in Roll-to-Roll manufacturing system. *Scientific Reports* 15(1), 1–17.
- [25] Martin, C., Zhao, Q., Patel, A., Velasquez, E., Chen, D., Li, W., 2025. A review of advanced roll-to-roll manufacturing: system modeling and control. *Journal of Manufacturing Science and Engineering* 147(4), 041004.
- [26] Guo, X., Keivan, D., Syed, U., Qin, L., Zhang, H., Dullerud, G., Seiler, P., Hu, B., 2024. Controlagent: Automating control system design via novel integration of llm agents and domain expertise. *arXiv preprint arXiv:2410.19811*.
- [27] Zahedifar, R., Mirghasemi, S.A., Baghshah, M.S., Taheri, A., 2025. LLM-Agent-Controller: A Universal Multi-Agent Large Language Model System as a Control Engineer. *arXiv preprint arXiv:2505.19567*.
- [28] Cui, C., Liu, J., Feng, J., Hui, P., Ghias, A.M.Y.M., Zhang, C., 2024. Large language models based multi-agent framework for objective oriented control design in power electronics. *arXiv preprint arXiv:2406.12628*.
- [29] Cui, C., Liu, J., Hui, P., Lin, P., Zhang, C., 2025. GenControl: Generative AI-Driven Autonomous Design of Control Algorithms. *arXiv preprint arXiv:2506.12554*.
- [30] Bayat, A., Abate, A., Ozay, N., Jungers, R.M., 2025. LLM-Enhanced Symbolic Control for Safety-Critical Applications. *arXiv preprint arXiv:2505.11077*.
- [31] Li, S., Li, J., Xu, J., Chen, D., 2025. From natural language to certified H-infinity controllers: Integrating LLM agents with LMI-based synthesis. *arXiv preprint arXiv:2511.07894*.
- [32] Li, J., Li, S., Chen, D., 2025. AURORA: Autonomous updating of ROM and controller via recursive adaptation. *arXiv preprint arXiv:2511.07768*.
- [33] Garcia, C.I., DiBattista, M.A., Letelier, T.A., Halloran, H.D., Camelio, J.A., 2024. Framework for LLM applications in manufacturing. *Manufacturing Letters* 41, 253–263.
- [34] Li, Y., Zhao, H., Jiang, H., Pan, Y., Liu, Z., Wu, Z., Shu, P., Tian, J., Yang, T., Xu, S., et al., 2024. Large language models for manufacturing. *arXiv preprint arXiv:2410.21418*.
- [35] Xia, Y., Shenoy, M., Jazdi, N., Weyrich, M., 2023. Towards autonomous system: flexible modular production system enhanced with large language model agents. In: 2023 IEEE 28th International Conference on Emerging Technologies and Factory Automation (ETFA). IEEE, pp. 1–8.
- [36] Chen, C., Zhao, K., Leng, J., Liu, C., Fan, J., Zheng, P., 2025. Integrating large language model and digital twins in the context of industry 5.0: Framework, challenges and opportunities. *Robotics and Computer-Integrated Manufacturing* 94, 102982.
- [37] Yang, L., Luo, S., Cheng, X., Yu, L., 2025. Leveraging Large Language Models for Enhanced Digital Twin Modeling: Trends, Methods, and Challenges. *arXiv preprint arXiv:2503.02167*.
- [38] Liu, X., Erkoyuncu, J.A., Fuh, J.Y.H., Lu, W.F., Li, B., 2025. Knowledge extraction for additive manufacturing process via named entity recognition with LLMs. *Robotics and Computer-Integrated Manufacturing* 93, 102900.
- [39] Gautam, A., Aryal, M.R., Deshpande, S., Padalkar, S., Nikolaenko, M., Tang, M., Anand, S., 2025. IIoT-enabled digital twin for legacy and smart factory machines with LLM integration. *Journal of Manufacturing Systems* 80, 511–523.
- [40] Gill, M.S., Vyas, J., Markaj, A., Gehlhoff, F., Mercangöz, M., 2025. Leveraging LLM Agents and Digital Twins for Fault Handling in Process Plants. *arXiv preprint arXiv:2505.02076*.
- [41] Shelton, J.J., 1986. Dynamics of web tension control with velocity or torque control. In: 1986 American Control Conference. IEEE, pp. 1423–1427.
- [42] Martin, C., Patil, A., Li, W., Tanaka, T., Chen, D., 2025. Model Predictive Path Integral Control for Roll-to-Roll Manufacturing. *arXiv preprint arXiv:2510.06547*.